Copper-Zirconium Tungstate Composites Exhibiting Low and Negative Thermal Expansion Influenced by Reinforcement Phase Transformations

DORIAN K. BALCH and DAVID C. DUNAND

A fully-dense Cu-75 vol pct ZrW_2O_8 metal matrix composite was fabricated by hot isostatic pressing of Cu-coated ZrW_2O_8 particles. A small amount of the high-pressure γ-ZrW_2O_8 phase was created during the cooldown and depressurization following densification; near complete transformation to γ-ZrW_2O_8 was achieved by subsequent cold isostatic pressing. The thermal expansion behavior of the composite between 25 °C and 325 °C was altered by the cold isostatic pressing treatment, and also depended on the length of time that had passed between thermal cycles. The measured thermal expansion coefficients within specific temperature ranges varied from $-6 \cdot 10^{-6}$ K^{-1} to far above the thermal expansion coefficient of the copper matrix. The complex temperature-dependent expansion/contraction behavior could be justified by considering the evolution of phase transformations taking place in the ZrW_2O_8 phase, which were observed by *in-situ* synchrotron X-ray diffraction measurements.

I. INTRODUCTION

ZIRCONIUM tungstate (ZrW_2O_8) is a ceramic with a strongly negative coefficient of thermal expansion (CTE).[1-4] In contrast to most other ceramics exhibiting negative CTE,[4,5] the CTE of ZrW_2O_8 is isotropic and has a large negative magnitude (average CTE of $-7.2 \cdot 10^{-6}$ K^{-1}) over a wide range of temperature (-273 °C to 777 °C).[4] These unusual properties suggest the incorporation of ZrW_2O_8 into a metallic matrix, to create a metal matrix composite with very low CTE, which could be tailored to specific engineering applications. Such a composite could be used in electronic packaging applications where high thermal conductivities coupled with low CTE values matching that of silicon ($4.1 \cdot 10^{-6}$ K^{-1}) or alumina ($6.7 \cdot 10^{-6}$ K^{-1}) are desired.[6,7] Alternatively, a ZrW_2O_8-base composite could be designed to have a CTE of zero, *i.e.*, constant dimensions over a specified temperature range, which would be advantageous in metrology, precision optics, and space structures.[8] At lower metal content, a composite with negative CTE could be achieved, with applications for temperature compensation, *e.g.*, for optical Bragg gratings.[4] Also, ZrW_2O_8 additions have been shown to reduce the CTE of cement-sand mixtures, with potential application in temperature-compensated concrete.[9] Recently, it was demonstrated that hot-pressing could be used to create Cu-ZrW_2O_8 composites, provided processing temperature and time were maintained within a process window where chemical reaction between the two phases does not take place.[10]

The thermal expansion behavior of ZrW_2O_8 is complicated, however, by the fact that it undergoes two phase transformations from the α-phase stable at ambient temperature and pressure to (a) a high-temperature β-phase, formed at 155 °C and ambient pressure;[2] and (b) a high-pressure γ-phase, formed at ambient temperature and hydrostatic pressures between 200 and 400 MPa.[11] The CTEs of all three phases are negative, but vary in magnitude from $CTE_\alpha = -8.7 \cdot 10^{-6}$ K^{-1} to $CTE_\beta = -4.9 \cdot 10^{-6}$ K^{-1} to $CTE_\gamma = -1.0 \cdot 10^{-6}$ K^{-1}.[4] The α-β transition is reversible without hysteresis upon cooling below 155 °C, while the high-pressure γ-phase is metastable upon release of the hydrostatic pressure at ambient temperature and exists until heating above 117 °C at ambient pressure.[11] There is a -4.95 pct volume contraction associated with the $\alpha \rightarrow \gamma$ transformation, while the α-β transformation is second order and is thus not associated with a volume change. In an earlier study of a copper matrix composite with 50 to 60 vol pct ZrW_2O_8 particles, residual γ-ZrW_2O_8 present due to the combination of consolidation stresses and thermal mismatch stresses was found to transform on heating and cooling, leading to high effective CTE values.[8] These composites were subsequently studied by synchrotron X-ray diffraction, which assessed *in situ* the volume fraction and identity of the ZrW_2O_8 phases during thermal cycling.[12,13]

In the present study, we investigate the thermal expansion behavior of a Cu-ZrW_2O_8 composite containing 75 vol pct ceramic particles, with the intent of producing a material exhibiting near-zero or negative thermal expansion. The higher volume fraction as compared to previous studies[8,12,13] was chosen to reduce the internal mismatch stresses in the ceramic inducing the $\alpha \rightarrow \gamma$ transformation, in the absence of which CTE values near zero are expected for the present composite. Processing, characterization, and dilatometry are presented, as are ceramic phase fraction synchrotron X-ray diffraction measurements made *in situ* during one thermal cycle of the composite.

II. EXPERIMENTAL METHODS

A. *Processing, Characterization, and Dilatometry*

ZrW_2O_8 powders (from Teledyne Wah Chang, Albany, OR) were crushed in a mortar and pestle and sieved to a size range of 25 to 106 μm; the majority of the particles were between 50 and 90 μm. The sieved particles were coated with high-purity (>99.9 pct) copper (performed at

DORIAN K. BALCH, Postdoctoral Appointee, is with the Engineered Materials Department, Sandia National Laboratories, Livermore, CA 94551. DAVID C. DUNAND, Professor, is with the Department of Materials Science and Engineering, Northwestern University, Evanston, IL 60208. Contact e-mail: dunand@northwestern.edu
Manuscript submitted May 9, 2003.

Advanced Ceramics Corp., Cleveland, OH) to a nominal thickness of 2.7 μm, corresponding to a copper volume fraction of approximately 25 pct. The coated particles were hot isostatic pressed (HIPed) (performed at the Michigan Technological University, Houghton, MI) at 500 °C and 200 MPa for 3 hours. This combination of temperature and time has been shown to minimize undesirable reactions while still allowing densification.[8,10]

Metallographic and dilatometric samples were sectioned using a low-speed diamond saw and polished with SiC paper and diamond suspensions. The parallelepiped dilatometry samples ranged in length from 10 to 20 mm with other dimensions between 3 and 5 mm; the faces perpendicular to the long dimension were parallel to within 10 μm. Some samples were cold isostatic pressed (CIPed) at 300 MPa for 49 hours, to convert as much of the ZrW_2O_8 as possible to the γ-phase. This was done to start both the dilatometry and diffraction experiments with an (ideally) fully γ-phase composite, rather than a mixture of α- and γ-phase in unknown proportions, as in previous studies.[8,12,13] Dilatometry was carried out on as-HIPed and CIPed samples in a calibrated dilatometer (Orton Model 1600, Westerville, OH) ramped at 2 °C/min between room temperature and 325 °C and back to room temperature, with a 30-minute hold at 325 °C. Densities of the as-HIPed, CIPed, and thermally cycled materials were measured by helium pycnometry.

B. Diffraction Experiment

The synchrotron diffraction study was performed at the DuPont-Northwestern-Dow Collaborative Access Team (DND-CAT) at Sector 5 of the Advanced Photon Source (APS, Argonne National Laboratory, IL). The general setup for these experiments has been described in detail in Reference 14. The sample was placed within a custom-built resistive furnace with two windows for the incoming and outgoing X-rays and with thermocouple instrumentation. The temperature of the composite was varied from room temperature to 233 °C and back in steps of 10 °C to 20 °C; for each temperature, the sample was exposed for 600 seconds to a monochromatic 65 keV (λ = 0.019 nm) X-ray beam with a square cross section of 0.5 × 0.5 mm. The Debye–Scherrer diffraction cones from the ZrW_2O_8 particles present in the diffraction volume of ~0.39 mm^3 were recorded using a CCD camera (from MAR Inc., Evanston, IL). Also recorded was the {110} Debye–Scherrer cone from a molybdenum powder standard at ambient temperature for calibration purposes. The CCD camera was situated at a distance of 1165 mm from the sample and 540 mm from the molybdenum standard, and had a 132-mm-diameter detector with 16-bit intensity capability over an orthogonal array of 2048 × 2048 pixels, each 64.4 by 64.4 μm.

III. RESULTS

The microstructure of the as-HIPed composite is shown in Figure 1. The volume fraction of copper, determined using image analysis software (Scion Image, from Scion Corporation, Frederick, MD), is 26.1 pct. There is some porosity evident both within ZrW_2O_8 particles (small rounded holes) and within the matrix (irregular holes). The volume fractions of ZrW_2O_8 particles and large irregular holes are 66.5 and

7.4 pct. There is no visible difference in the microstructure of the CIPed or thermally cycled material. The densities measured by pycnometry were 5.94, 6.28, and 5.92 g/cm^3 for the as-HIPed, CIPed, and thermally cycled samples, respectively.

Dilatometry curves for both as-HIPed and CIPed samples are shown in Figures 2 through 4. Figure 2 shows one thermal cycle (heating and cooling) for the as-HIPed material and two thermal cycles for the material that had been CIPed at 300 MPa. Figure 3 shows in greater detail the cooling portion of the first cycle and the entire second cycle of the CIPed composite. Figure 4 shows two additional thermal cycles on the same as-HIPed and CIPed samples shown in Figure 2, carried out 16 months after the initial set of thermal cycles (Figure 2); the period of 16 months was a result of external constraints, and was not chosen deliberately. Listed in Table 1 are measured secant CTEs of various portions of each curve.
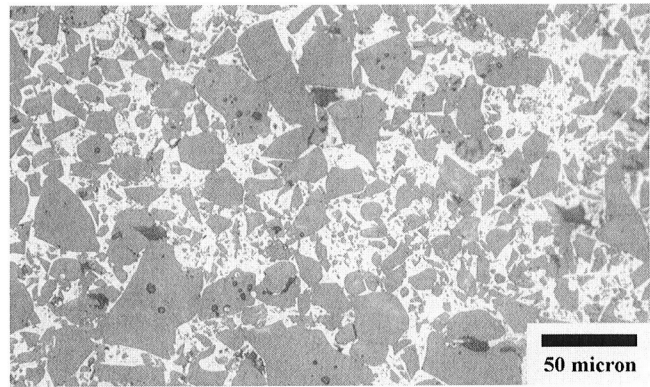

Fig. 1—Optical micrograph of as-HIPed composite. Light phase is the copper matrix, gray phase is the ZrW_2O_8 reinforcement, and irregular dark patches are particle pullouts.
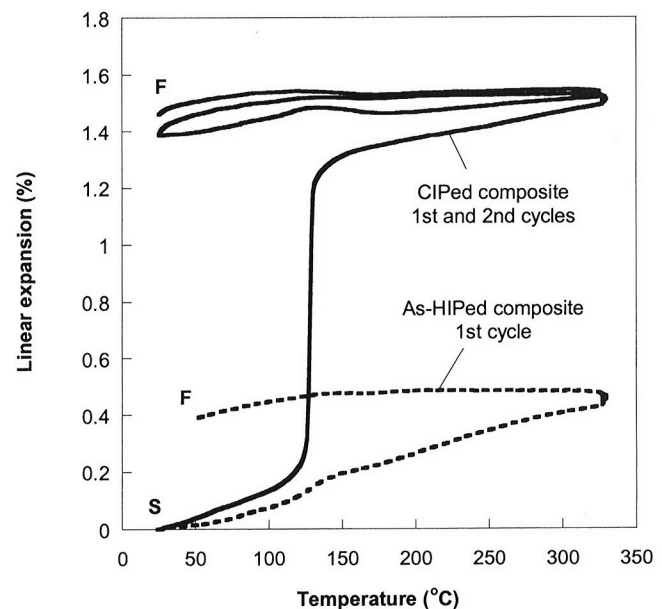

Fig. 2—Dilatometry of as-HIPed (first thermal cycle) and CIPed (first and second thermal cycles) composites. Start and finish are marked by "S" and "F," respectively.
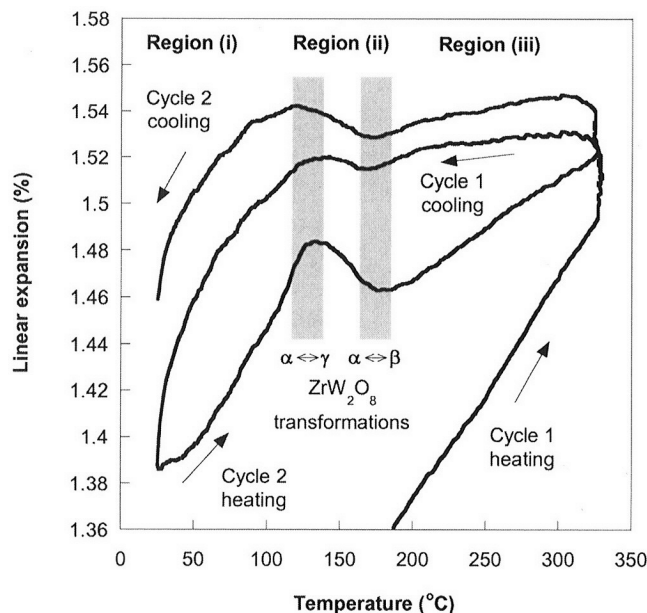
Fig. 3—Dilatometry of CIPed composite, cooling of first cycle and all of second cycle. The temperature ranges in which ZrW_2O_8 phase transformations occur are marked with gray bars. Regions (i) to (iii) are discussed in Section IV–B.
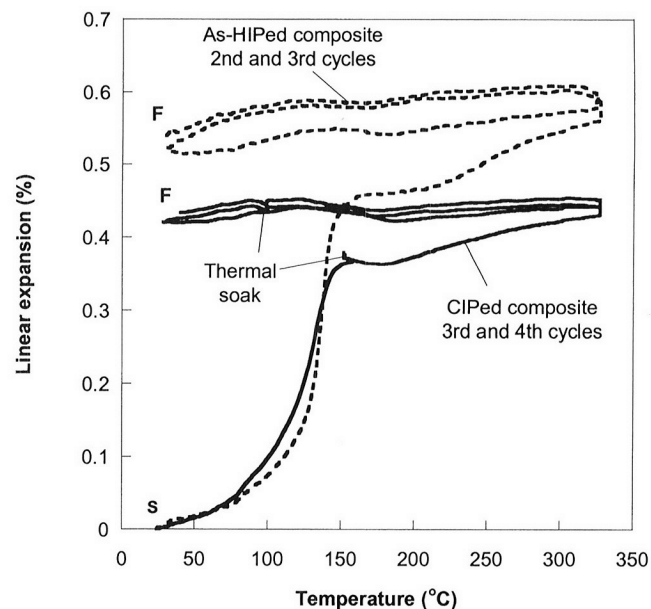

Fig. 4—Dilatometry of as-HIPed (second and third thermal cycles) and CIPed (third and fourth thermal cycles) composites, performed 16 months after cycles shown in Fig. 2.

Table I. Experimental Secant CTE Values (10^{-6} K^{-1})

Interval (°C)	Initial Cycles (Figure 2)			Subsequent Cycles (Figure 4)*			
	As-HIPed Cycle 1	CIP Cycle 1	CIP Cycle 2	As-HIPed Cycle 2	As-HIPed Cycle 3	CIP Cycle 3	CIP Cycle 4
Heating							
25 to 100	9.9	17.6	7.7	9.5	1.7	12.9	2.0
140 to 160	15.6	25.7	−6.0	45.6	−0.30	18.7	−0.94
200 to 300	14.3	9.4	4.4	7.9	2.7	4.8	1.6
50 to 300	15.6	57.2	4.6	21.0	2.3	16.2	0.75
Cooling							
300 to 200	−0.34	0.64	1.1	1.2	1.4	0.99	1.2
160 to 140	0.31	−1.8	−3.6	−0.55	−1.1	−2.5	−2.2
100 to 50	11.7	8.9	6.4	6.1	5.0	2.6	2.7
50 to 30	**	19.4	13.6	10.6	8.9	3.8	**
300 to 50	3.7	2.8	1.6	2.4	2.1	0.64	0.67

*Measured 16 months after initial cycles.
**Not measured.

In all dilatometric experiments, there was a half-hour hold at 325 °C prior to cooling; in cycles 3 and 4 of the CIPed material (Figure 4), 1-hour holds also occurred at various intermediate temperatures. The slight expansions seen during these holds are artifacts caused by the sample holder and pushrod reaching thermal equilibrium slightly later than the samples, and were also seen with a pure copper sample. The cooling data are still expected to be quite accurate, as the final sample lengths measured by micrometer at the end of cooling cycles were in excellent agreement with those calculated from the dilatometric curves.
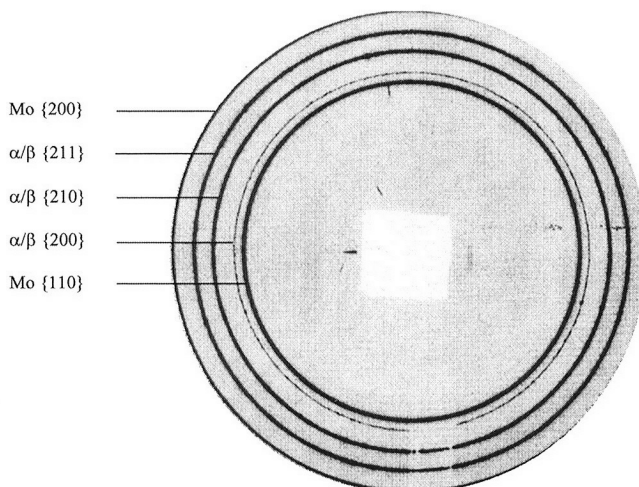
Figure 5(a) shows a synchrotron X-ray diffraction pattern of an as-CIPed sample (without prior dilatometric cycling) taken at 25 °C, with the following rings visible (from innermost to outermost): γ-phase {011}, {031}, and {131}; Mo {110}; γ-phase {060}, {201} + {160} + {032}, and

{231} + {161} + {132}; and Mo {200}. The γ-phase triplets correspond to crystallographic planes whose d-spacings differ by less than 0.005 nm; as these rings could not be resolved, their combined intensities were analyzed as a single ring. Figure 5(b) shows a pattern for the same sample at 193 °C, where all γ-phase rings have disappeared and the following rings are now visible (from inside to outside): Mo {110}; α/β-phase {200}, {210}, and {211}; and Mo {200}. No crystallographic distinction can be made between rings of α-phase and β-phase ZrW_2O_8, as there is no significant change in the unit cell lattice parameter during the second-order α-β transformation. The rings corresponding to the cubic ZrW_2O_8 phases will therefore be referred to as α/β in the following discussion.

Figure 6(a) shows the intensity as a function of temperature for the α/β and γ rings between room temperature and
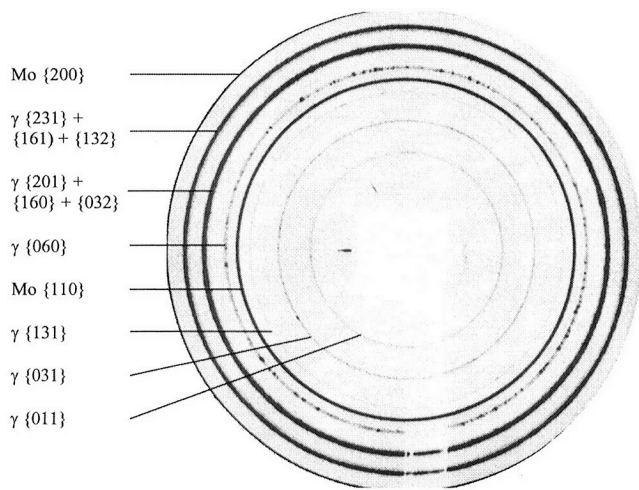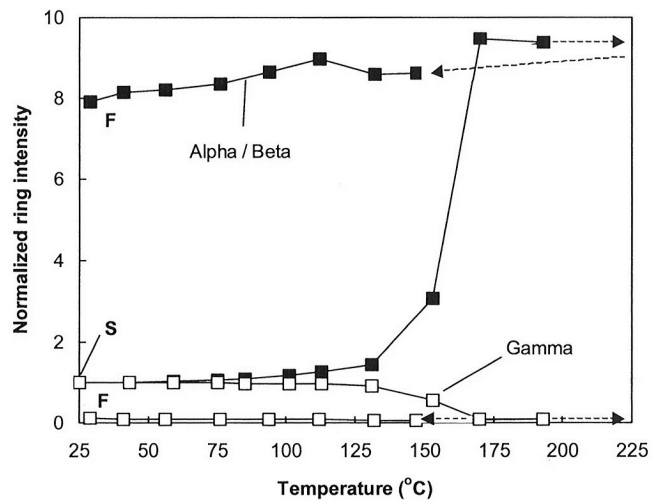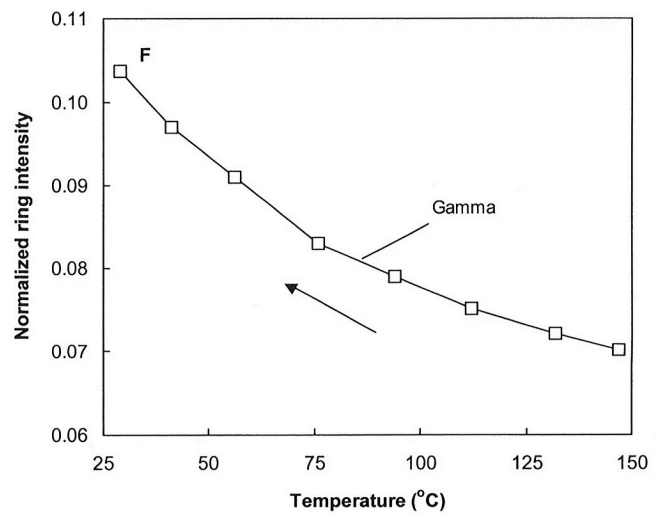
(a)

(b)

Fig. 5—(*a*) Synchrotron X-ray diffraction pattern of CIPed composite at 25 °C. (*b*) Synchrotron X-ray diffraction pattern of CIPed composite at 193 °C.

(a)

(b)

Fig. 6—(*a*) Normalized diffracted intensities of α/β- and γ-ZrW_2O_8 as a function of temperature during the first cycle of CIPed composite. Dashed arrows indicate heating between 193 °C and 233 °C, and cooling between 233 °C and 147 °C, during which acquired intensity data were unreliable. (*b*) Normalized diffracted intensities of γ-ZrW_2O_8 as a function of temperature during cooling between 147 °C and 29 °C of CIPed composite.

193 °C during heating and between 147 °C and 29 °C during cooling, normalized to the room-temperature intensity. Intensity calculations were performed by summation of pixel intensities within concentric bands corresponding to specific diffraction peaks from different phases. This was followed by background subtraction and division by the number of pixels counted for each band, to obtain average intensity values independent of the background intensity or the radius of each analysis band. The reference powder standard was placed "downstream" of the sample (*i.e.*, out of the heated zone), and its diffraction ring was used, together with the output of an ionization chamber placed "upstream" of the sample, to normalize the diffracted intensities for any fluctuations in X-ray flux and sample positioning. As this standard was placed "downstream" of the sample, there is slight shadowing of the sample rings, seen at the bottom of each pattern (Figures 5(a) and (b)); this small angular region was not included in the intensity calculations.

No data points are shown in Figure 6 for the temperature range 193 °C → 233 °C → 147 °C, due to partial shifting of

the sample out of the X-ray beam in this temperature interval. This was caused by thermal expansion mismatch between the sample and the steel sample holder, and was detected by a sharp increase in the intensity of the diffracted rings from the downstream calibration standard. Repositioning of the sample prior to the 147 °C cooling exposure restored the calibration ring intensities to their expected values. Figure 6(b) shows the intensity as a function of temperature of the γ-ZrW_2O_8 ring between 147 °C and 29 °C during cooling.

IV. DISCUSSION

A. *Microstructure*

The densities of copper, α-ZrW_2O_8, and γ-ZrW_2O_8 are 8.94, 5.072, and 5.355 g/cm^3, respectively.[15,16] Based on the 66.5 pct volume fraction for ZrW_2O_8 determined by metallography, the densities for composites containing all of the ZrW_2O_8 phase

in the α- or γ-phases are calculated as 5.71 and 5.89 g/cm³, respectively. These values are sufficiently below the measured densities (5.94 and 6.28 g/cm³) for the as-HIPed and CIPed samples to suggest that the large voids seen in Figure 1 are due to particle pullout during polishing. Assuming a ZrW_2O_8 volume fraction of 73.9 pct (the sum of the ZrW_2O_8 and porosity volume fractions), the predicted densities are 6.08 and 6.29 g/cm³, much closer to the measured values. This volume fraction of 73.9 pct is also close to the nominal value of 75 pct calculated from the thickness of copper deposited on the particles. We thus conclude that the composite ZrW_2O_8 volume fraction was approximately 75 pct. The large increase in density measured after CIPing is strongly indicative of the majority of the ZrW_2O_8 being transformed to the γ-phase, as also expected from the CIP pressure (300 MPa), shown to be sufficient to induce the γ-phase transformation in pure ZrW_2O_8.[11] We then conclude that the CIPed material contained mostly γ-phase ZrW_2O_8.

B. Dilatometry

Figure 2 shows the thermal expansion behavior during the initial thermal cycles of both the as-HIPed (first cycle) and CIPed (first and second cycles) material. The behavior of the as-HIPed material is similar to that measured for a HIPed composite with 60 vol pct ZrW_2O_8 in previous work:[8] an initial region of fairly high CTE ($\sim 10 \cdot 10^{-6}$ K⁻¹), followed by a region of increased expansion between 120 °C and 150 °C due to the 4.95 pct volume expansion during the $\gamma \rightarrow \alpha$ phase transformation. Continued expansion to 325 °C with a CTE around $15 \cdot 10^{-6}$ K⁻¹ is followed by cooling with a near-zero ($0.5 \cdot 10^{-6}$ K⁻¹) CTE until approximately 130 °C is reached, below which the CTE increases to over $10 \cdot 10^{-6}$ K⁻¹. This anomalous contraction is again interpreted as being due to thermal stresses initiating the $\alpha \rightarrow \gamma$ phase transition.

The CIPed material exhibits a markedly different behavior during its first thermal cycle, where the initial high-CTE region between 25 °C and 120 °C is followed by a sharp and large expansion between 120 °C and 140 °C, associated with the $\gamma \rightarrow \alpha$ phase transformation. As virtually all of the ZrW_2O_8 is expected to be γ-phase after CIPing, the upper bound (isostrain approximation) for the expected composite expansion due to this transformation is $1/3 \cdot f \cdot \Delta V/V = 1.24$ pct (based on a volume fraction $f = 0.75$ and a volume expansion $\Delta V/V = 4.95$ pct). A more rigorous elastic Eshelby micromechanical calculation,[17,18,19] incorporating the matrix and reinforcement volume fractions, elastic constants, and temperature-dependent thermal expansion coefficients,[11,20] and assuming isotropic behavior of the ceramic with a Poisson's ratio of 0.25, typical for oxide materials,[21] predicts an expansion of 1.14 pct, in excellent agreement with the measured expansion of 1.13 pct and lending support to the assumption of 100 pct transformation to γ-ZrW_2O_8 during CIPing.

Continued expansion of the CIPed material to 325 °C occurs with a CTE close to $10 \cdot 10^{-6}$ K⁻¹, while the cooling curve and second thermal cycle show three distinct regions, as marked in Figure 3: (i) room temperature to $\sim$120 °C, with fairly high (8.6 to $13.3 \cdot 10^{-6}$ K⁻¹) CTE; (ii) $\sim$140 °C to 160 °C, with sharply negative (-1.8 to $-6.0 \cdot 10^{-6}$ K⁻¹) CTE, and (iii) $\sim$175 °C to 325 °C, with low (0.7 to $4.3 \cdot 10^{-6}$ K⁻¹), but positive, CTE. These regions can be assigned to (i) presence of α-ZrW_2O_8 with a small amount of γ-ZrW_2O_8 formation

due to the compressive thermal residual stress the copper matrix exerts upon the ZrW_2O_8, (ii) presence of 100 pct α-ZrW_2O_8 in the region between the $\alpha \leftrightarrow \gamma$ and $\alpha \leftrightarrow \beta$ phase transformations (marked by gray bars in Figure 3), and (iii) presence of β-ZrW_2O_8 above the $\alpha \leftrightarrow \beta$ transition temperature. We can therefore claim limited success in reaching our goal of achieving low or negative CTE, but only within regions (ii) and (iii), as the thermal stress-induced formation of the relatively high ($-1.0 \cdot 10^{-6}$ K⁻¹) CTE γ-ZrW_2O_8 below approximately 120 °C, combined with the volume contraction associated with the $\alpha \rightarrow \gamma$ transformation, results in composite thermal expansion closer to that of the copper matrix.

Figure 4 shows the expansion behavior of the same as-HIPed and CIPed samples, each subjected to two additional thermal cycles performed 16 months after the cycling shown in Figure 2. Despite the difference in the starting states of these samples, after the initial cycling (Figure 2) and room-temperature storage, both samples exhibit very similar behavior: heating through a $\gamma \rightarrow \alpha$ phase transformation that causes approximately 0.35 pct linear expansion, followed by behavior very similar to that shown in Figure 3. Regardless of the starting state of these materials, heating to 325 °C "homogenizes" the phase fractions and stress states in the composites. Subsequent cycling results in near-zero (2 to $4 \cdot 10^{-6}$ K⁻¹) overall CTE between room temperature and 325 °C, with negative CTE in the region where only α-ZrW_2O_8 is present. During extended storage at room temperature, the residual compressive stress in the ZrW_2O_8 from the previous cycle drives the $\alpha \rightarrow \gamma$ transformation over time, as reported in neutron diffraction experiments studying the transformation in pure ZrW_2O_8;[11] similarly sluggish stress-induced transformation at room temperature has been observed in stabilized zirconia composites.[22] On the basis of the Cα 0.35 pct linear expansion, it is estimated that $\sim$30 pct of the ZrW_2O_8 transforms to the γ-phase over time.

The initial engineering goal of this study was to produce composites with uniform thermal expansion behavior, which could be tailored to meet specific application requirements. The thermal expansion results discussed here are clearly lacking in uniformity, due primarily to the effect of the very large volume change during the $\gamma \rightarrow \alpha$ phase transformation. In order to produce composites with a stable CTE over a wide temperature range, one of two approaches could be pursued.[8] The first is to use a matrix with a very low yield stress and minimal propensity to strain harden under repeated thermomechanical loading; this would prevent the average stresses in the ZrW_2O_8 from reaching the levels required to induce the transformation. The second approach would be to use an alternate negative CTE ceramic reinforcement that does not undergo phase transformations involving large volume changes at stresses reachable within a metallic matrix. Hafnium tungstate, HfW_2O_8,[23] and zirconium molybdenate, $ZrMo_2O_8$,[24] both show promise in this regard, but present new processing issues (hygroscopic behavior, lower decomposition temperature, and unknown compatibility with Cu) that must be addressed before they can be used as composite reinforcements.

C. Diffraction Experiment

Synchrotron X-rays have been used for in-situ investigations of phase fractions present in metals and intermetallics under thermal loading.[25,26] Figures 6(a) and (b) show the intensities

of the α/β- and γ-phase peaks during heating and cooling of an as-CIPed sample. The intensities are normalized to the initial intensity; *i.e.*, at 193 °C the intensity of the α/β rings is approximately 9.4 times greater than their intensity at 25 °C, while the γ-phase rings are approximately 15 times less intense. The values shown are the averages of values calculated for the two most intense reflections of each phase: the α/β {210} and {211} rings, and the γ {201} + {160} + {032} and {231} + {161} + {132} triplets. The other rings, although visible, are too faint to be reliably analyzed.

The intensities of the α/β rings start to increase above 100 °C, with a concurrent decrease in the γ-phase intensities. There is a sharp increase in α/β intensity between 130 °C and 170 °C, to values over 9 times greater than the initial value, while the γ-phase intensity drops to near zero. This is in excellent agreement with the interpretation of the dilatometry data obtained on the as-CIPed material (Figure 2). The intensity of the α/β rings slowly decreases with cooling, while there is a small but noticeable increase in the γ intensity near room temperature, as seen in Figure 6(b). Due to beamline time constraints, repeated measurements at room temperature after cooling were not made; these measurements could have confirmed the slow growth of γ-ZrW_2O_8 over time driven by the residual stresses in the composite.

The preceding results are in general agreement with a very recent diffraction study performed on a Cu-60 vol pct ZrW_2O_8 composite.[12,13] The present study differs on the following points: (1) the use of uncycled (*i.e.*, not previously thermally cycled) material; (2) the use of an external powder standard for intensity calibration; (3) reliable knowledge of the initial ZrW_2O_8 phase fractions; (4) *ex-situ* calibration of the thermocouple/furnace system using a thin-foil thermocouple bonded to the surface of a composite sample; (5) optimized choice of sample to detector distance, to separate the α/β- and γ-phase diffraction rings; and (6) use of temperature-dependent CTE values for both Cu and ZrW_2O_8 during modeling, rather than average values taken over broad temperature ranges.

V. CONCLUSIONS

A copper matrix composite containing 75 vol pct ZrW_2O_8 was fabricated by hot isostatic pressing of copper-coated ceramic particles, with the intention of making a composite with near-zero coefficient of thermal expansion and high thermal conductivity. Stress-induced formation of the high-pressure γ-phase of ZrW_2O_8 was unavoidable, however, and had a significant effect on the composite CTE. Thermal expansion of both the as-HIPed and CIPed composites were of greater magnitude than expected during heating, due to the volume expansion of ZrW_2O_8 associated with the $\gamma \rightarrow \alpha$ phase transformation. During cooling, regions of alternating positive and negative CTE were recorded, corresponding to the transformation of ZrW_2O_8 from the high-temperature β-phase to the low-temperature α-phase around 160 °C, followed by partial transformation to the high-pressure γ-phase as thermal mismatch stresses increased near room temperature. A second thermal cycle performed immediately after the first yielded curves similar to the first cooling curve. Synchrotron X-ray diffraction provided direct confirmation of these transformations during the first thermal cycle of the CIPed composite.

Thermal cycling performed 16 months later resulted again in a sharp increase in length on heating, while subsequent cooling exhibited similar behavior to that seen during the first cooling experiment. Again, immediate subsequent cycling gave a near stable behavior. These results can be explained by the slow formation of approximately 30 pct of γ-phase ZrW_2O_8 under the action of residual stresses generated by the previous thermal cycling, followed by rapid back-transformation on heating.

In summary, dilatometry and *in-situ* X-ray diffraction can explain the complex CTE behavior of these composites. The heating curves vary widely depending on the amount of γ-phase present, which can be produced by residual stresses due to fabrication (HIPing), compression at room temperature (CIPing), or thermal mismatch upon long-term storage at room temperature. Once the γ-phase has been transformed on heating, near-zero CTE values are achieved, provided the γ-phase does not reappear as a result of thermal mismatch stresses. A different choice of matrix material, to minimize thermal stresses, or negative-CTE reinforcement, to minimize stress-induced phase transformations, may produce stable, uniform, and tailorable low or negative CTE behavior in this class of composite materials.

REFERENCES

1. C. Martinek and F.A. Hummel: *J. Am. Ceram. Soc.*, 1968, vol. 51, pp. 227-28.
2. J.S.O. Evans, T.A. Mary, T. Vogt, M.A. Subramanian, and A.W. Sleight: *Chem. Mater.*, 1996, vol. 8, pp. 2809-23.
3. T.A. Mary, J.S.O. Evans, T. Vogt, and A.W. Sleight: *Science*, 1996, vol. 272, pp. 90-92.
4. A.W. Sleight: *Ann. Rev. Mater. Sci.*, 1998, vol. 28, pp. 29-43.
5. C.N. Chu, N. Saka, and N.P. Suh: *Mater. Sci. Eng.*, 1987, vol. 95, pp. 303-08.
6. C. Zweben: *JOM*, 1992, vol. 44, pp. 15-23.
7. C. Zweben: *JOM*, 1998, vol. 50, pp. 47-51.
8. H. Holzer and D.C. Dunand: *J. Mater. Res.*, 1999, vol. 14, pp. 780-89.
9. M. Kofteros, S. Rodriguez, V. Tandon, and L.E. Murr: *Scripta Mater.*, 2001, vol. 45, pp. 369-74.
10. C. Verdon and D.C. Dunand: *Scripta Mater.*, 1997, vol. 36, pp. 1075-80.
11. J.D. Jorgensen, Z. Hu, S. Teslic, D.N. Argyriou, S. Short, J.S.O. Evans, and A.W. Sleight: *Phys. Rev. B*, 1999, vol. 59, pp. 215-25.
12. S. Yilmaz: *J. Phys: Cond. Matter*, 2002, vol. 14, pp. 365-75.
13. S. Yilmaz: *Compos. Sci. Technol.*, 2002, vol. 62, pp. 1835-39.

14. A. Wanner and D.C. Dunand: *Metall. Mater. Trans. A*, 2000, vol. 31A, 2949-62.
15. *Metals Handbook*, 10th ed, ASM international, Materials Park, OH, 1990, vol. 2.
16. *Zirconium Tungstate Property Sheet*, Wah-Chang, Albany, OR, 1996.
17. J.D. Eshelby: *Proc. R. Soc. A*, 1957, vol. 241, pp. 376-96.
18. Y. Benveniste: *Mech. Mater.*, 1987, vol. 6, pp. 147-57.
19. T.W. Clyne and P.J. Withers: *An Introduction to Metal Matrix Composites*, Cambridge University Press, Cambridge, United Kingdom, 1993.
20. *Handbook of Elastic Properties of Solids, Liquids, and Gases*, M. Levy, H.E. Bass, and R.R. Stern, eds., Academic Press, San Diego, CA, 2001, vol. II.
21. D.J. Green: *An Introduction to the Mechanical Properties of Ceramics*, Cambridge University Press, Cambridge, United Kingdom, 1998.
22. V. Sergo and D.R. Clarke: *J. Am. Ceram. Soc.*, 1995, vol. 78, pp. 641-44.
23. J.D. Jorgensen, Z. Hu, S. Short, A.W. Sleight, and J.S.O. Evans: *J. Appl. Phys.*, 2001, vol. 89, pp. 3184-88.
24. C. Lind, A.P. Wilkinson, Z.B. Hu, S. Short, and J.D. Jorgensen: *Chem. Mater.*, 1998, vol. 10, pp. 2335-37.
25. S.O. Svensson, G. Vogl, M. Kaisermayr, and A. Kvick: *Acta Mater.*, 1997, vol. 45, pp. 4205-12.
26. A. Schuster, H. Voggenreiter, D.K. Balch, and D.C. Dunand: *Mater. Res. Soc. Symp. Proc.*, 2001, vol. 678, pp. EE2.6.1-EE2.6.6.